Journal of Thermal Analysis and Calorimetry, Vol. 78 (2004) 687–695

INVESTIGATION OF IrO_2/SnO_2 THIN FILM EVOLUTION BY THERMOANALYTICAL AND SPECTROSCOPIC METHODS

E. Horváth[1*], *J. Kristóf*[2], *R. L. Frost*[3], *N. Heider*[2] *and V. Vágvölgyi*[2]

[1]Department of Environmental Engineering and Chemical Technology, University of Veszprém, H-8201 Veszprém, P.O.Box 158, Hungary
[2]Department of Analytical Chemistry, University of Veszprém, H-8201 Veszprém, P.O.Box 158, Hungary
[3]School of Physical and Chemical Sciences, Queensland University of Technology, 2 George Street, GPO Box 2434, Brisbane, Qld. 4001, Australia

Abstract

The formation mechanism of thermally prepared IrO_2/SnO_2 thin films has been investigated under in situ conditions by thermogravimetry combined with mass spectrometry (TG-MS) and infrared emission spectroscopy (IRES). Mixtures of varying composition of the precursor salts ($SnCl_2\cdot 2H_2O$ dissolved in ethanol and $IrCl_3\cdot 3H_2O$ dissolved in isopropanol) were prepared onto titanium metal supports. Then the solvent was evaporated and the gel-like films were heated in an atmosphere containing 20% O_2 and 80% Ar to 600°C. The thermogravimetric curves showed that the evolution of the oxide phases take place in several decomposition stages and the final mixed oxide film is formed between 490 and 550°C, depending on the noble metal content.

Mass spectrometric ion intensity curves revealed that below 200°C crystallization water, residual solvent, and hydrogen-chloride (formed as a result of an intramolecular hydrolysis) are liberated. The decomposition of surface species (surface carbonates, carbonyls and carboxylates) formed via the interaction of the residual solvent with the precursor salts takes place up to 450°C as evidenced by emission Fourier transform infrared spectrometry.

Keywords: infrared emission spectroscopy, IrO_2, SnO_2, sol-gel process, TG-MS, thin films

Introduction

Dimensionally stable anodes (DSA®) as binary mixtures of a Group VIII noble-metal oxide and a stabilizing oxide deposited on a base metal are widely used in the electrochemical industry from the 1960s [1]. One of the new fields in the development of oxide anodes is their application in oxygen evolution conditions such as galvanics, metal electrowinning, electroflotation, organic electrosyntheses, cathode protection, etc. [2–5]. The anodic stability and the service life are among the most critical conditions for DSAs. IrO_2 is the most important active component of high performance an-

---

[*] Author for correspondence: E-mail: elizabet@almos.vein.hu

1388–6150/2004/ $ 20.00

Akadémiai Kiadó, Budapest
Kluwer Academic Publishers, Dordrecht

odes due to its high corrosion resistivity. The stability of IrO_2 can be further improved by the addition of stabilizing agents like TiO_2, Ta_2O_5, Nb_2O_5 and SnO_2 [6]. It was found that a mixed metal oxide anode of the composition 70% Ir and 30% Ta is considered to be the best performing electrode in oxygen evolution processes [7–10].

SnO_2 thin films are also of widespread interest because of their favourable properties like optical transparency over the visible wavelengths and high chemical and thermal stability. They are widely used for detection of oxidizing and reducing gases, as well [11–13].

Listed among the parameters influencing electrochemical performance are the film thickness, grain size and porosity which can be controlled during the preparation. Surface morphology and structural effects influence the catalytic properties independent of the methods of preparation. The sol-gel technique has several advantages over other methods of preparation such as low-cost processing, easy control of film thickness and porosity, as well as the ability to produce porous structures consisting of ultra-fine particles offering a large specific surface area [14]. The flexibility of this method is also of high importance when the kinetics of phase formation has to be controlled, and when second or third components has to be added.

In the present study the thermal evolution process of IrO_2/SnO_2 coatings prepared by the sol-gel technique on a titanium metal support was followed by the combination of thermal analysis and mass spectrometry. The surface composition of the heated films was monitored by Fourier transform infrared emission spectrometric (IRES) analysis.

Experimental

Thin film preparation

In order to follow the thermal evolution process of IrO_2/SnO_2 thin films, the $IrCl_3{\cdot}3H_2O$ precursor (Fluka, Buchs, Switzerland) was dissolved in isopropanol and the $SnCl_2{\cdot}2H_2O$ one (Sigma-Aldrich, Budapest, Hungary) was dissolved in ethanol and a 0.05 M stock solution was prepared for each component. Mixtures of varying composition of the precursor salts (varied from 10% Ir to 100% Ir with 10% Ir steps) were prepared by the sol–gel method onto titanium metal supports (size 4×4 mm, thickness 0.1 mm) etched in boiling oxalic acid (10%), washed with distilled water, rinsed with acetone, and dried at room temperature. The coating was prepared by applying the precursor solution drop-by-drop onto the support and removing the solvent by hot air (70–80°C). This procedure was continued until a measurable quantity of the film (2–5 mg) corresponding to a 400–700 nm thick layer was formed.

Thermoanalytical investigation

The heat treatment of the gel-like coatings was carried out in Netzsch TG 209 - type thermobalance in a gas atmosphere containing 20% oxygen and 80% argon at a heating rate of $10°C\ min^{-1}$. To follow the evolution of the gaseous products over the temperature range from 20 to 600°C, the thermobalance was connected to a Balzers MSC 200 - type mass spectrometer. The transfer line for delivering the gaseous decomposition products into the mass spectrometer was a fused silica capillary temperature controlled to 150°C.

Fourier transform infrared emission spectroscopic (IRES) analysis

The surface composition of the heated films was monitored as a function of the firing temperature by means of a Bio-Rad FTS-60A type FTIR spectrometer which was modified by replacing the IR source with an emission cell. The infrared emission cell consists of a modified atomic absorption graphite rod furnace driven by a thyristor-controlled AC power source capable of delivering up to 150 ampers at 12 volt. A platinum sheet acts as a hot plate to heat the sample on top. An insulated type R thermocouple was embedded inside the platinum sheet to control the temperature. The operating temperature was controlled to ±2°C using a Eurotherm Model 808 type proportional temperature controller. The emission spectra were collected at 50°C intervals in the 100–600°C range. The spectra were acquired by coaddition of 64 scans at a resolution of 4 cm^{-1}.

Results and discussion

The thermogravimetric (TG) and the derivative thermogravimetric (DTG) curves of $IrCl_3$ and $SnCl_2$ containing gels of varying composition are shown in Fig. 1. By comparing the curves, it can be concluded that the $IrCl_3$ component decomposes at the highest temperature (a straight line in the TG curve can only be observed over 580°C) in several – at least five – mass loss stages. A detailed study on the formation mechanism of IrO_2 coatings by the sol-gel method has already been made [15]. On the contrary, the thermal events of the $SnCl_2$ gel seem to be finished by about 350°C. As to the thermal behaviour of the two-component systems, a monotonous change can be seen as a function of the changing composition.

Since the best-performing electrode of the IrO_2/Ta_2O_5 system contains 30% stabilizing agent, the thermal behaviour of the analogous system was studied in detail. The thermogravimetric (TG) and the derivative thermogravimetric (DTG) curves of 4.31 mg gel containing 70 mol% $IrCl_3$ and 30 mol% $SnCl_2$ on a titanium metal support are given in Fig. 2. By comparing the curves, four different regions can be distinguished in the DTG trace as follows: from ambient to 150°C, between 150 and 300°C, from 300 to 400°C, and from 400 to 550°C. In the first mass loss range three overlapping stages can be observed at 60, 104 and 125°C. According to earlier studies [15] crystallization water and residual solvent is released from the gel-like film in this temperature range. The liberation of this latter component is evidenced by the ion intensity curve m/z =43 ($C_2H_3O^+$ fragment ion) given in Fig. 3. Since a small amount of the solvent is present in the coating even up to 200°C, it can be supposed that some interaction (e.g. chemisorption or complexation) between the precursor salts and the solvent takes place. According to experience, no water can be detected when chlorine, or hydrogen chloride is formed simultaneously. This is due to the formation of

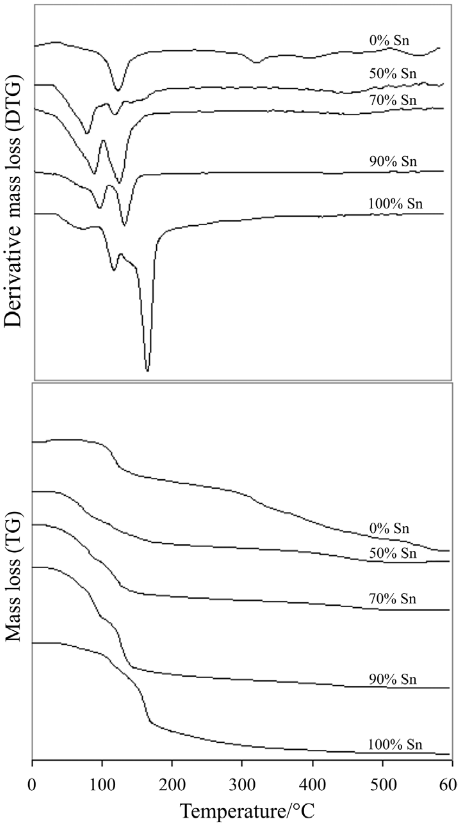

Fig. 1 TG and DTG curves of $IrCl_3$ and $SnCl_2$ containing gels of varying composition on titanium metal support

hydrochloric acid adsorbing strongly to the silica capillary wall. (The difficulties associated with the coupling of a thermobalance to a mass spectrometer was recently discussed in detail [16]. Some times, the complexity of a film formation reaction necessitates the use of evolved gas analysis by FT-IR as well [17]). It was reported earlier that hydrogen chloride is formed at low temperature when a hydrated iridium chloride film is heated [18]. It was stated that an intramolecular hydrolysis takes place, simultaneously with the liberation of crystallization water, resulting in the formation of iridium oxychloride and hydrogen chloride according to the equation

$$IrCl_3 + H_2O = IrOCl + 2HCl$$

Since a substantial amount of crystallization water was removed by the evaporating solvent during the preparation of the coating, the reduction of the water content reduces the extent of hydrolysis, as well. The formation of chlorinated species in the first region of thermal events can also be supported by the ion intensity curve $m/z = 70$ (Cl_2^+ ion) in Fig. 3.

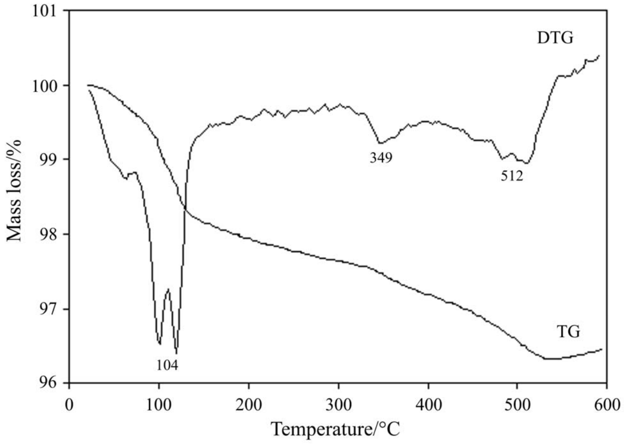

Fig. 2 TG and DTG curves of the coating containing 70% $IrCl_3 \cdot 3H_2O$ and 30% $SnCl_2 \cdot 2H_2O$

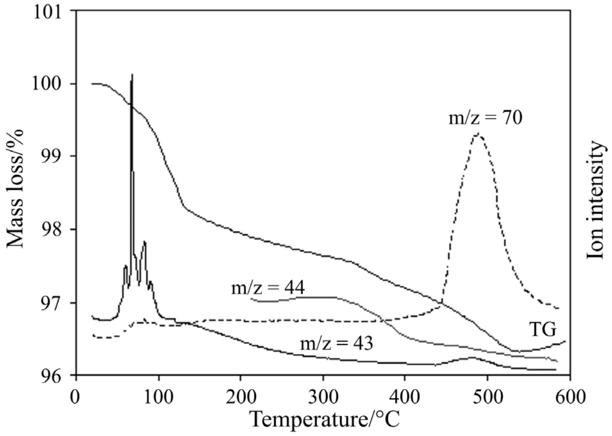

Fig. 3 TG and mass spectrometric ion intensity curves of the coating containing 70% $IrCl_3 \cdot 3H_2O$ and 30% $SnCl_2 \cdot 2H_2O$ ($m/z = 70$: $^{35}Cl_2^+$, $m/z = 44$: CO_2^+, $m/z = 43$: $C_2H_3O^+$)

In the temperature range between 150 and 300°C a monotonous decrease can be observed in the TG curve. The ion intensity curve $m/z = 70$ (Cl_2^+ ion) shows the evolution of chlorine gas at a constant, low rate. A more intense chlorine formation can only be observed over 400°C. The thermal decomposition process between 300 and 400°C (with maximum rate at 349°C in the DTG curve) is due – in addition to chlorine evolution of low intensity – to the decomposition of organic surface species formed between the metal ions in the film and the solvent alcohol. The formation of carbon dioxide as evidenced by the ion intensity curve $m/z = 44$ (CO_2^+ ion) in Fig. 3 is a proof of a combustion process. The nature of the surface species found will be discussed later on.

The liberation of the major amount of chlorine gas (and the formation of the final mixed oxide film as defined by the temperature at which a straight line is obtained in the TG curve) takes place between 400 and 550°C. It is interesting to observe that a small amount of residual solvent trapped in the film is also formed as shown by the ion intensity curve of the $C_2H_3O^+$ fragment ion ($m/z = 43$). Due to the high intensity gas formation (chlorine liberation) in the final stage of solidification/oxide formation, a highly porous film is expected to form. This can be an advantage because an electrode coating of high specific surface area can be obtained. Over 550°C a slight increase can be observed in the TG curve due to the partial oxidation of the titanium metal support. Since titanium oxide is an *n*-type semiconductor, the firing temperature should not exceed 600°C.

In order to completely characterize the process of film evolution, the composition of the solid phase should also be monitored as a function of the firing temperature. The change of the surface composition of a black, porous film on a metal support can only be followed by infrared emission spectroscopy, when the infrared source is the heated sample itself. Figure 4 shows the change of the IR spectrum as a function of the firing temperature. The assignment of the bands found are summarized in Table 1. At low temperatures the emitted intensity is inherently low, therefore the spectra are rather noisy, especially in the high wavenumber range. The signal to noise ratio is significantly improved over 200°C. At 100°C the band at 974 cm^{-1} belongs to the out-of-plane O–H vibration of residual alcohol. With the increase of the temperature the intensity of this band decreases gradually and a new peak is emerging in this range at around 800 cm^{-1} due to metal-oxygen vibrations. The band at 1215 cm^{-1} can be assigned as CH_2 twisting, while the one at 1599 cm^{-1} is a composite band consisting of carboxylate stretching and water deformation vibrations. The most interesting feature of the spectra is the high intensity C–O stretching band at 2123 cm^{-1}. Since this band cannot be observed in the diffuse reflectance (DRIFT) spectra of the transparent SnO_2 films, it can be concluded that a metal carbonyl is present in the film, or more likely a terminal $-C\equiv C$, up to 450°C. This is in perfect harmony with the TG-MS data of Fig. 3. The formation of CO_2 in the 300–450°C range is due to the combustion of CO released from the film.

In the higher frequency range C–H stretching bands (3086 cm^{-1}) and a broad O–H stretching band (3300–3600 cm^{-1}) can be observed. Since the intensity of the O–H stretching band is increasing with the increase of the tin content in the heated films, it can be concluded that $-Sn(OH)_2-O-Sn(OH)_2-O-$ type polymer chains are formed in which the OH groups remain stable even at elevated temperatures [19–22]. High-temperature water evolution from tin-oxide containing thin films using tin-chloride hydrate precursor was also reported [23].

Both the thermoanalytical and the infrared patterns of the films with varying composition show a gradual change as a function of the SnO_2 composition. Thus, the conclusion can be made that the two oxide phases develop independently. This change, however, is not a linear one as indicated by the DTG peak temperature of the final chlorine evolution step or the final temperature of film solidification (at which the TG curve becomes straight) as shown in Fig. 5. In order to reveal the possible in-

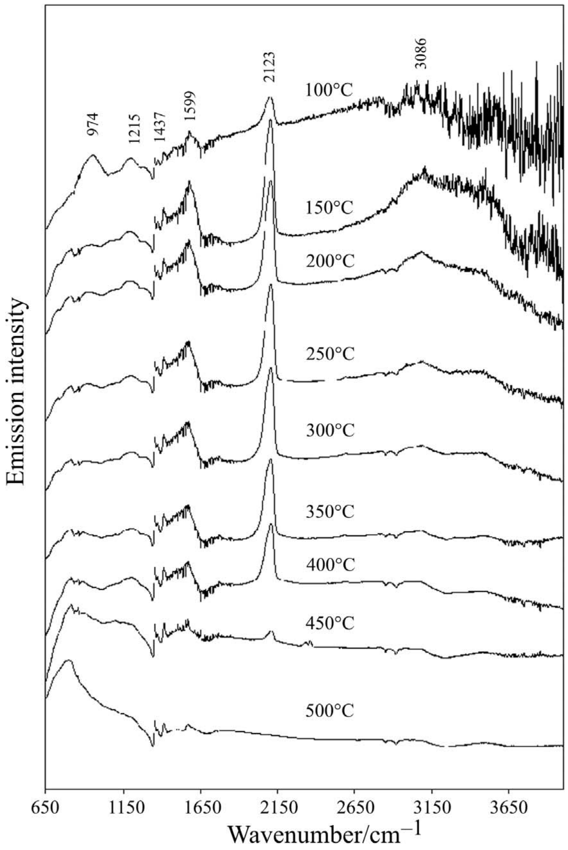

Fig. 4 Infrared emission spectra of the coating containing 70% $IrCl_3 \cdot 3H_2O$ and 30% $SnO_2 \cdot 2H_2O$ heated to different temperatures

Table 1 Assignment of IR bands of the film containing 70% $IrCl_3 \cdot 3H_2O$ and 30% $SnCl_2 \cdot 2H_2O$ heated to different temperatures

Band position/cm^{-1}	Assignment	Description
3300–3600	ν_{OH}	O–H stretching
2950–3200	ν_{CH}	C–H stretching
2000–2200	$\nu_{(CO)x}$	C–O stretching
1600–1610	β_{H_2O}	water deformation
1550–1630	$\nu_{(COO^-)}$	carboxylates streching
1000–1300	γ_{CH_2}	CH_2 twisting
880–1000	γ_{OH} , δ_{CH_3}	out-of-plane OH, CH_3 rocking
650–850	$\nu_{M–O}$	oxide bands

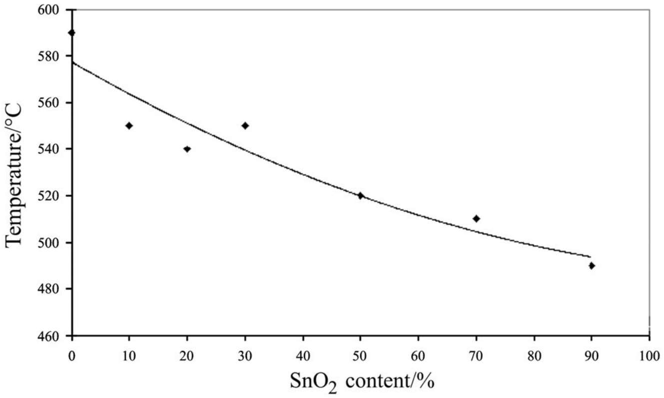

Fig. 5 Change of the final film formation temperature as a function of the SnO_2 content

teraction between the two oxide phases, further studies are necessary e.g. with secondary ion mass spectrometry (SIMS) or wide-angle X-ray scattering (WAXS).

Conclusions

Thermogravimetry combined with mass spectrometry is an indispensable tool to follow thin film evolution reactions of complicated nature via the continuous monitoring of gas phase composition. For a more complete characterization of the formation process, however, this technique has to be complemented with infrared emission spectroscopy capable of monitoring the surface composition of the films as a function of the temperature. Although this technique was rarely practiced in the past, its importance is growing significantly in applications involving the development of thin films and different types of coating materials.

* * *

This research was supported by the Hungarian Scientific Research Fund under Grant OTKA T 034355. The financial and infrastructural support of the Inorganic Materials Research Program of the Queensland University of Technology is also gratefully acknowledged.

References

1 S. Trasatti (Ed.), Electrodes of Conductive Metal Oxides, Elsevier, Amsterdam, Part A, 1980; Part B, 1981.
2 F. Cardarelli, P. Taxil, A. Savall, Ch. Comninellis, G. Manoli and O. Leclerc, J. Appl. Electrochem., 28 (1998) 245.
3 S. Trasatti, Electrochim. Acta, 45 (2000) 2377.
4 M. Morimitsu, H. Tamura, M. Matsunaga and R. Otogawa, J. Appl. Electrochem., 30 (2000) 511.
5 C. Bock, H. Spinney and B. MacDougall, J. Appl. Electrochem., 30 (2000) 523.
6 L. K. Xu and J. D. Scantlebury, Corrosion Sci., 45 (2003) 2727.

7 R. Mraz and J. Krysa, J. Appl. Electrochem., 24 (1994) 1262.
8 Ch. Comninellis and G. P. Vercesi, J. Appl. Electrochem., 21 (1991) 335.
9 J. Rolewicz, Ch. Comninellis, E. Plattner and J. Hinden, Electrochim. Acta, 33 (1988) 573.
10 L. K. Xu and J. D. Scantlebury, J. Electrochem. Soc., 150 (2003) B254.
11 W. Gobel and K. D. Schierbaum, Sens. Actuat. B-Chem, 26/27 (1995) 1.
12 P. P. Tsai, I. C. Chen and M. H. Tzeng, Sens. Actuat. B-Chem, 24/25 (1995) 537.
13 A. Chaturvedi, V. N. Mishra, R. Dwivedi and S. K. Srivastava, Microel. J., 30 (1999) 259.
14 B. Gautheron, M. Labeau, G. Delabougliser and U. Schmatz, Sens. Actuat. B-Chem, 15/16 (1993) 357.
15 J. Kristóf, J. Liszi, P. Szabó, A. Berbieri and A. De Battisti, J. Appl. Electrochem., 23 (1993) 615.
16 K. Mészáros-Szécsényi, J. Päiväsaari, M. Putkonen, L. Niinistö and G. Pokol, J. Therm. Anal. Cal., 69 (2002) 65.
17 M. Krunks, J. Madarász, T. Leskelä, A. Mere, L. Niinistö and G. Pokol, J. Therm. Anal. Cal., 72 (2003) 497.
18 J. Kristóf, J. Mihály, S. Daolio, A. De Battisti, L. Nanni and C. Piccirillo, J. Electroanal. Chem., 434 (1997) 99.
19 N. Chiondini, F. Meinardi, A. Paleari, R. Scotti and G. Spinolo, Solid State Commun., 109 (1999) 145.
20 H. Yunpu, L. Yadong, Y. Juan and Q. Yitai, Mater. Lett., 40 (1999) 823.
21 B. Thangaraju, Thin Solid Films, 402 (2002) 71.
22 A. Cabot, A. Diezguez, A. Romano-Rodriguez, J. R. Morate and N. Barsan, Sens. Actuat. B-Chem, 79 (2001) 98.
23 S. Seki, T. Aoyama, Y. Sawada, M. Ogawa, M. Sano, N. Miyabayashi, H. Yoshida, Y. Hoshi, M. Ide and A. Shida, J. Therm. Anal. Cal., 69 (2002) 1021.